

---

# VARIATIONAL QUANTUM CIRCUITS FOR DEEP REINFORCEMENT LEARNING

---

**Samuel Yen-Chi Chen**  
Department of Physics  
National Taiwan University  
Taipei, Taiwan  
ycchen1989@gmail.com

**Chao-Han Huck Yang**  
School of ECE  
Georgia Institute of Technology  
Atlanta, GA, USA  
huckiyang@gatech.edu

**Jun Qi**  
School of ECE  
Georgia Institute of Technology  
Atlanta, GA, USA  
jq41@gatech.edu

**Pin-Yu Chen**  
IBM Research  
Yorktown Heights, NY, USA  
pin-yu.chen@ibm.com

**Xiaoli Ma**  
School of ECE  
Georgia Institute of Technology  
Atlanta, GA, USA  
xiaoli@gatech.edu

**Hsi-Sheng Goan**  
Department of Physics  
National Taiwan University  
Taipei, Taiwan  
goan@phys.ntu.edu.tw

## ABSTRACT

The state-of-the-art Machine learning approaches are based on classical Von-Neumann computing architectures and have been widely used in many industrial and academic domains. With the recent development of quantum computing, a couple of tech-giants have attempted new quantum circuits for machine learning tasks. However, the existing quantum machine learning is hard to simulate classical deep learning models because of the intractability of deep quantum circuits. Thus, it is necessary to design approximated quantum algorithms for quantum machine learning. This work explores variational quantum circuits for deep reinforcement learning. Specifically, we reshape classical deep reinforcement learning algorithms like experience replay and target network into a representation of variational quantum circuits. On the other hand, we use a quantum information encoding scheme to reduce the number of model parameters as small as the scale of  $\text{poly}(\log N)$  in contrast to  $\text{poly}(N)$  in a standard configuration. Besides, our variational quantum circuits can be deployed in many near-term noisy intermediate quantum machines.

**Keywords** Quantum signal processing · variational quantum Circuits · deep reinforcement learning · quantum computation · communication network

## 1 Introduction

Deep Learning (DL) [1] has been widely used in many machine learning domains, such as computer vision [2, 3, 4], natural language processing [5], communication network congestion control [6], and mastering the game of Go [7]. The successful deployment of DL is primarily attributed to the improvement of new computer architectures associated with powerful computing capabilities in the past decades. With a recent development of quantum computing, many machine learning work start to consider techniques of quantum mechanics such as quantum many-body physics[8, 9, 10], phase-transitions [11], quantum control [12, 13], and quantum error correction [14, 15] because those methods can be used for machine learning data analysis. Although quantum computing machines have been brought to the market by a few technological companies (e.g., IBM’s and D-Wave’s hardware solutions [16, 17].) However, a large scale of quantum circuits cannot be faithfully employed upon the quantum computing platforms due to the lack of quantum error correction [18, 19]. Therefore, our work designs approximate quantum algorithms and encoding schemes [20] on the devices with noise tolerance. More specifically, we take the advantages of quantum entanglement [20, 21] in quantum computing to reduce our model size into an essentially small number such that quantum algorithms can be realized on the available quantum platforms which are named as Noisy Intermediate-Scale Quantum machines (NISQ).

By taking the strengths of quantum computing on NISQ with significantly fewer parameters, variational quantum circuits on NISQ have succeeded in implementing standard classification and clustering algorithms on classical benchmark datasets. Besides, NISQ based quantum computation enables us to employ quantum circuits for implementing new DL algorithms like generative adversarial networks [22] (GAN). However, to our best knowledge, variational circuit on current NISQ quantum computing for deep neural network based decision making and policy selection have not discussed, which constrains the application of NISQ in many machine learning scenarios with continuous time frames.

Since reinforcement learning (RL) and deep reinforcement learning (DRL) are two potential issues and satisfy the requirements of automatic policy learning under uncertainty, our work focuses on the empowerment of DRL on NISQ quantum computation, which refers to an agent interacting with the environment to gain a knowledge of backgrounds and deriving the policy of decision making accordingly. [23, 24]. Furthermore, we generalize variational quantum circuits to standard DRL based *action-value* function approximation [24, 25].

Finally, we propose a novel variational quantum circuit on the current NISQ platform to resolve the circuit challenges. Besides, we analyze the policy reward and the memory cost for performance of our NISQ based DRL in comparison with standard RL and DRL approaches.

## 2 Methods

### 2.1 Reinforcement Learning

*Reinforcement learning* is a machine learning paradigm in which an *agent* interacts with the *environment*  $\mathcal{E}$  over a number of discrete time steps [23]. At each time step  $t$ , the agent receives a *state* or *observation*  $s_t$  and then chooses an *action*  $a_t$  from the set of possible actions  $\mathcal{A}$  according to its *policy*  $\pi$ . The policy is a function mapping the state  $s_t$  to action  $a_t$ . After executing the action  $a_t$ , the agent receives the state of the next time step  $s_{t+1}$  and a scalar *reward*  $r_t$ . The process continues until the agent reaches the terminal state. An *episode* is defined as an agent starting from a randomly selected initial state and following the aforementioned process all the way through the terminal state.

Define  $R_t = \sum_{t'=t}^T \gamma^{t'-t} r_{t'}$  as the total discounted return from time step  $t$ , where  $\gamma$  is the discount factor that lies in  $(0, 1]$ . In principle,  $\gamma$  is provided by the investigator to control how future rewards are given to the decision making function. When a large  $\gamma$  is concerned, the agent takes into account future rewards no matter what a discount rate is; As to a small  $\gamma$ , an agent can quickly ignore future rewards within a few time steps. The goal of the agent is to maximize the expected return from each state  $s_t$  in the training process. The *action-value function* or *Q-value function*  $Q^\pi(s, a) = \mathbb{E}[R_t | s_t = s, a]$  is the expected return for selecting an action  $a$  in state  $s$  based on policy  $\pi$ . The optimal action value function  $Q^*(s, a) = \max_\pi Q^\pi(s, a)$  gives a maximal action-value across all possible policies. The value of state  $s$  under policy  $\pi$ ,  $V^\pi(s) = \mathbb{E}[R_t | s_t = s]$ , is the agent's expected return by a following policy  $\pi$  from the state  $s$ .

#### 2.1.1 Q-Learning

Q-learning [23] is a model-free RL algorithm. Before the learning process begins,  $Q$  is initially assigned to an arbitrary fixed value (chosen by the programmer). Then, at each time, the agent selects an action  $a_t$ , observes a reward  $r_t$ , enters a new state  $s_{t+1}$  (that may depend on both the previous state  $s_t$  and the selected action), and then  $Q$  is updated.

$$Q(s_t, a_t) \leftarrow Q(s_t, a_t) + \alpha [R_{t+1} + \gamma \max_a Q(s_{t+1}, a) - Q(s_t, a_t)]. \quad (1)$$

#### 2.1.2 SARSA

An SARSA [23] agent interacts with the environment and updates the policy based on the undertaking actions. In other words, it is known as an online policy learning algorithm. The  $Q$  value for a state-action is updated by an error, adjusted by the learning rate  $\alpha$ .  $Q$  values represent the possible reward received in the next time step for taking action  $a$  in state  $s$ , plus the discounted future reward received from the next state-action observation:

$$Q(s_t, a_t) \leftarrow Q(s_t, a_t) + \alpha [R_{t+1} + \gamma Q(s_{t+1}, a_{t+1}) - Q(s_t, a_t)] \quad (2)$$

#### 2.1.3 Deep Q-Learning

The action-value function  $Q(s, a)$  can be explicitly represented by a two-dimensional table with a total number of entries  $s \times a$ . However, when the state space or the action space is large or even continuous the tabular method is

unfeasible. In such a situation, the action-value function is represented with function approximators such as neural networks [24, 25].

The employment of neural networks for function approximators to represent the  $Q$ -value function has been studied extensively [24, 25] and succeeded in many tasks like playing video games. In this setting, the action-value function  $Q(s, a; \theta)$  is parameterized by  $\theta$ . The  $\theta$  can be derived by a series of iterations from a variety of optimization methods adapted from other machine learning tasks. The simplest form is the  $Q$ -learning. In this method, the goal is to directly approximate the optimal action-value function  $Q^*(s, a)$  with the loss function:

$$L(\theta) = \mathbb{E}[(r_t + \gamma \max_{a'} Q(s', a'; \theta^-) - Q(s, a; \theta))^2] \quad (3)$$

The target is  $r_t + \gamma \max_{a'} Q(s', a'; \theta^-)$  and the prediction is  $Q(s, a; \theta)$ , where  $s'$  is the state encountered after playing action  $a_t$  at state  $s$ .

Since DRL is normally hard to converge, it is likely to get diverged when a nonlinear approximator like a neural network is used to represent the action-value function [25]. There are several possible culprits: When the states or observations are serially correlated with each other along the trajectory, thereby violating the assumption that the sample needs to be independent and identically distributed (IID), the  $Q$  function changes dramatically and changes the policy at a relatively large scale. In addition, the correlation between the action-value  $Q$  and the target values  $r_t + \gamma \max_{a'} Q(s', a')$  can be large. Unlike the supervised learning where the targets are given and invariant, the setting of deep reinforcement learning allows targets vary with  $Q$ , causing the  $Q$  to chase a nonstationary target.

The *deep Q-learning* presented in the work [25] addressed these issues through two mechanisms:

- *Experience replay*: To perform experience replay, we store each transition the agent encounters. The transition is stored as a tuple in the following form:  $(s_t, a_t, r_t, s_{t+1})$  at each time step  $t$ . To update the  $Q$ -learning parameters, we randomly sample a batch of experiences from the replay memory and then perform gradient descent with the following loss function:  $L(\theta) = \mathbb{E}_{\text{replaybatch}}[(r + \gamma \max_{a'} Q(s', a'; \theta^-) - Q(s, a; \theta))^2]$ . The key importance of experience replay is to lower the correlation of inputs for training the  $Q$ -function.
- *Target Network*:  $\theta^-$  is the parameter of the target network and these parameters are only updated at every finite steps. This setting helps to stabilize the  $Q$ -value function training since the target is relatively stationary compared to the action-value function.

## 2.2 Variational Quantum Circuits

The variational quantum circuit is one type of quantum circuits with tunable parameters which need to be optimized in an iterative manner. These parameters can be seen as the *weights* in artificial neural networks. Due to the lack of quantum error correction and fault-tolerant quantum computing in the near-term quantum devices, these variational circuits can be relatively robust against noises because the related deviations can be absorbed by the parameters during the iterative optimization process. Therefore, the machine learning algorithms powered by variational quantum circuits can circumvent the complex quantum errors which exist in the available quantum devices. Previous works [26, 20, 27] have demonstrated that the variational circuits can model any function approximators, classifiers and even quantum-many-body physics that are intractable on classical computers. For example, the work [20] shows that a variational quantum circuits can approximate an analytical function  $f(x)$ . It is hard to simulate the quantum circuits with large number of qubits via classical computers, which implies that the variational quantum circuits own a better expressive power than the classical function approximators like a neural network.

## 2.3 Variational Quantum Deep Q Learning

In this work, we attempt to expand the expressive power of variational quantum circuits for the action-value function. The variational quantum circuits require fewer parameters than a conventional neural network, making them promising for modeling complex environments. For a *target network*, we construct two sets of circuit parameters with the same circuit architecture. The targeted circuit is updated per 20 steps. For *experience replay*, the replay memory is set for the length of 80 to adapt to the testing environment *Frozen-Lake* and length of 1000 for *Cognitive Radio*, and the size of training batch is 5 for all of the environments. The process of optimization needs to calculate gradients of expectation values of quantum measurements, which can be conducted by the same circuit architecture and slightly different parameters, respectively [28]. Further, we encode the state with *computational basis encoding*. In the *Frozen-Lake* environments, there are totally 16 states. Thus, it requires 4 qubits to represent all states. In the *Cognitive-Radio* experiments, we apply similar method and circuit architectures with different number of qubits to match the number of possible channels Figure2. Besides, [29] provides a general discussion about the different encoding schemes.

---

**Algorithm 1** Variational Quantum Deep Q Learning
 

---

```

Initialize replay memory  $\mathcal{D}$  to capacity  $N$ 
Initialize action-value function circuit  $Q$  with random parameters
for episode = 1,  $M$  do
    Initialise state  $s_1$ 
    for  $t = 1, T$  do
        With probability  $\epsilon$  select a random action  $a_t$ 
        otherwise select  $a_t = \max_a Q^*(s_t, a; \theta)$ 
        Execute action  $a_t$  in emulator and observe reward  $r_t$  and next state  $s_{t+1}$ 
        Store transition  $(s_t, a_t, r_t, s_{t+1})$  in  $\mathcal{D}$ 
        Sample random minibatch of transitions  $(s_j, a_j, r_j, s_{j+1})$  from  $\mathcal{D}$ 
        Set  $y_j = \begin{cases} r_j & \text{for terminal } s_{j+1} \\ r_j + \gamma \max_{a'} Q(s_{j+1}, a'; \theta) & \text{for non-terminal } s_{j+1} \end{cases}$ 
        Perform a gradient descent step on  $(y_j - Q(s_j, a_j; \theta))^2$ 
    end for
end for
    
```

---

### 2.3.1 Computational Basis Encoding

For a general  $n$ -qubit state, it can be represented as:

$$|\psi\rangle = \sum_{(q_1, q_2, \dots, q_n) \in \{0,1\}^n} c_{q_1, \dots, q_n} |q_1\rangle \otimes |q_2\rangle \otimes |q_3\rangle \otimes \dots \otimes |q_n\rangle, \quad (4)$$

where  $c_{q_1, \dots, q_n} \in \mathbb{C}$  is the *amplitude* of each quantum state and each  $q_n \in \{0, 1\}$ .

The square of the amplitude is the *probability* of measurement with the output  $|q_1\rangle \otimes |q_2\rangle \otimes |q_3\rangle \otimes \dots \otimes |q_n\rangle$  and the total probability should sum to 1.

$$\sum_{(q_1, q_2, \dots, q_n) \in \{0,1\}^n} \|c_{q_1, \dots, q_n}\|^2 = 1 \quad (5)$$

For example, there are 16 possible states in the environment *Frozen-Lake*. Each possible state is labeled with an integer in the range from 0 to 15. The encoding procedure is as the following: The *decimal* number is first converted into a *binary* number and then encoded into the quantum states through single qubit unitary rotation. In other words, each quantum state can be denoted by a four-digit binary number  $b_1 b_2 b_3 b_4$ , where  $b_1, b_2, b_3, b_4$  can only take the value of 0 or 1. Therefore, the encoded quantum state is  $|b_1\rangle \otimes |b_2\rangle \otimes |b_3\rangle \otimes |b_4\rangle$ . For example, the *state* observed by the agent, 12, is first converted to the binary number 1100, which will be  $|1\rangle \otimes |1\rangle \otimes |0\rangle \otimes |0\rangle$ .

We propose the following single qubit unitary rotation method to encode the classical states from the testing environments into the quantum circuits Fig1. The rotation angles are:

$$\begin{aligned} \theta_i &= \pi \times b_i \\ \phi_i &= \pi \times b_i \end{aligned}$$

where  $i$  represents the index of each qubit. In this work, the total number of qubits is 4; therefore, the index is the set  $\{1, 2, 3, 4\}$ .

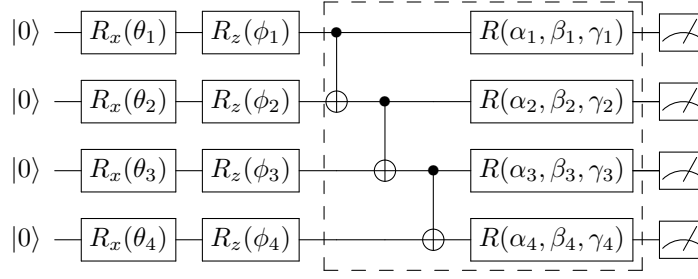


Figure 1: **Generic circuit architecture for the deep reinforcement learning.** This is the generic variational quantum circuit architecture for deep  $Q$  learning. The parameters labeled  $\theta$  and  $\phi$  are for state preparation and are not subject to iterative optimization. The CNOT gates are used to entangle quantum states from each qubit. Parameters labeled  $\alpha$ ,  $\beta$  and  $\gamma$  are the ones for iterative optimization. Note that the grouped box may repeat several times to increase the number of parameters. The number of qubits can be adjusted to fit the problem of interest and the capacity of the simulators of quantum machines. In this work, the grouped circuit repeats two times and therefore the total number of circuit parameters subject to optimization is  $4 \times 3 \times 2 = 24$ . It is often to add a bias after the quantum measurement, the length of the bias vector is the same as the number of qubits. The bias vector is also subject to optimization. Therefore, the total number of parameters in this example is  $24 + 4 = 28$

## 2.4 Quantum Circuit for Radio Network

In the experiments on the *cognitive radio*, the total number of channels that can be selected by the agent at each time-step is known in advance. Since the channel changes from time to time, it is necessary to include not only the *channel* but also the *temporal* information into the observation. The *observation* is in the following form:  $(channel, time)$ . Let the number of channel is  $N$ , there are  $N$  time-steps in a full channel-changing cycle. The number of possible states is thus  $N^2$ . In addition, at each time-step, the agent can select one of the channel from the set of all possible channels, which is of number  $N$ . Given this scenario, classical  $Q$ -learning, which is tabular based, will have  $N^3$  entries in the table. In the neural network based deep  $Q$ -learning, the number of parameters will be  $2 \times N^2 + 2 \times N$  [30]. However, with our proposed variational quantum circuits, the number of circuit parameters is  $N \times (3 \times 2 + 1)$ , see Table3 and Figure6.

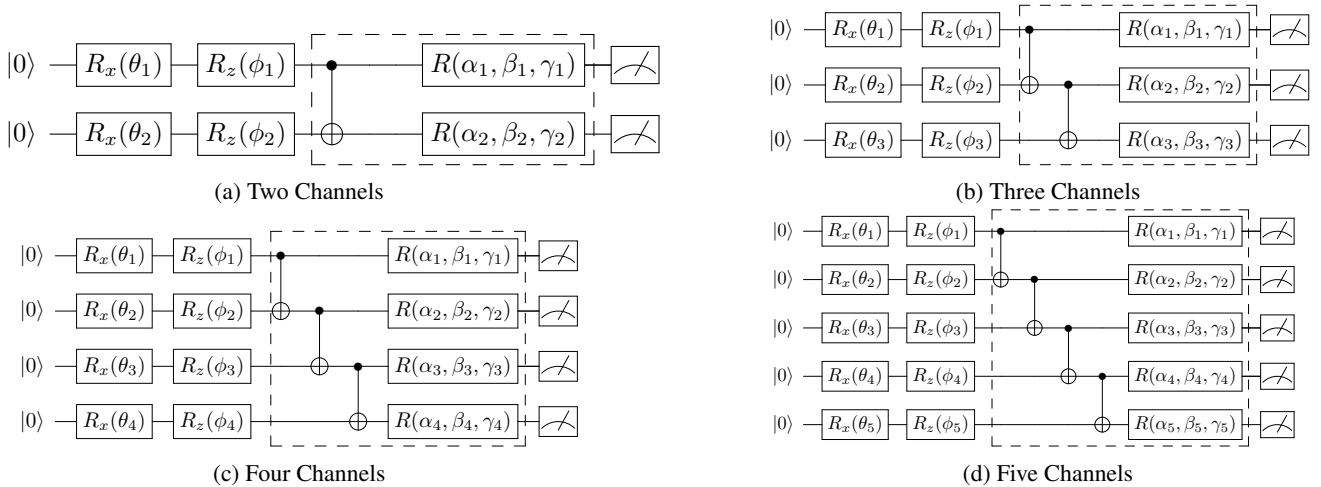


Figure 2: For circuit configurations for cognitive radio experiment.

## 3 Experiment and Results

### 3.1 Environment Setup

We set up the experiment following the circuit architecture in Fig1. The quantum circuit as shown in the figure is numerically simulated with the software package PennyLane [31]. We use the standard package PyTorch [32] to help the

Table 1: The list of reward in our testing environment Frozen-Lake and Cognitive Radio. In Frozen-Lake, the environment is non-slippery. Setting of this not only encourages the agent to achieve the goal but also encourages it to select the shortest path.

(a) Frozen-Lake		(b) Cognitive-Radio	
Location	Reward	Location	Reward
HOLE	-0.2	Occupied Channel	-1.0
GOAL	+1.0	Available Channel	+1.0
OTHER	-0.01		

linear algebraic manipulation to accelerate the simulation. OpenAI Gym [33] provides the testing environment. In this work, we choose an environment with low computational complexity, FrozenLake, to implement the proof-of-concept experiments. The FrozenLake environment mapping is:

- Observation: observed records of all time steps.
- Action: there are four actions in the action space. The outputs from the quantum circuit are 0, 1, 2, 3 and they correspond to the action LEFT, DOWN, RIGHT, UP
- Reward: The rewards in this environment are +1.0 for successfully achieve the goal, −0.2 for failing the task, which is stepping into the HOLE. Moreover, to encourage the agent to take the shortest path, there is also a −0.01 reward for each step taken.

### 3.2 Numerical Simulation

The optimization is chosen to be *RMSprop* with *learning rate* = 0.01, *alpha* = 0.99 and *eps* =  $10^{-8}$ , which is used widely in deep reinforcement learning. The batch-size for the experience replay is 5. The  $\epsilon$ -greedy strategy used in *Frozen-Lake* is the following:

$$\epsilon \leftarrow \frac{\epsilon}{\frac{episode}{100} + 1} \quad (6)$$

and in the environment *Cognitive-Radio* the  $\epsilon$  is updated in every single step as:

$$\epsilon \leftarrow 0.99\epsilon \quad (7)$$

with initial  $\epsilon = 1.0$  for encouraging more exploration in early episodes and shifting to more exploitation in later episodes.

### 3.3 Simulation with Noise

To investigate the robustness of our proposed variational quantum circuit-based RL against the noise from current and possible near-term devices. We perform the additional simulation which included the noises from the real quantum computer. The experiment setting is the same as the previous experiments, except that the simulation backend is replaced with the Qiskit-Aer simulation software, which has the capability to incorporate the noise model from the IBM quantum computers. The noise model data used in this work is stored at the GitHub repository.

### 3.4 Performance Analysis

In the Frozen-Lake experiment, we ran 500 episodes and the agent converged to reward 0.9 after the 198th episode, see Figure3. It is noted that, however, several sub-optimal results occurred. This phenomenon is probably due to the  $\epsilon$ -greedy policy selection. In the Cognitive-Radio experiment experiment, we tested situations where there are 2,3,4 and 5 possible channels for the agent to choose, respectively. In the all four situations, we ran 500 episodes and the agent converged to optimal at around 100 iterations, see Figure4. In the simulation with the noise model from the IBM quantum machine, the agent converged to optimal at around 100 iterations, which is comparable to previous ideal and noiseless simulations, showing that our proposed quantum circuit based RL is robust against noise in current machines. For the numerical simulation code and the parameters, please refer to the GitHub repository<sup>1</sup>.

<sup>1</sup><https://github.com/ycchen1989/Var-QuantumCircuits-DeepRL>

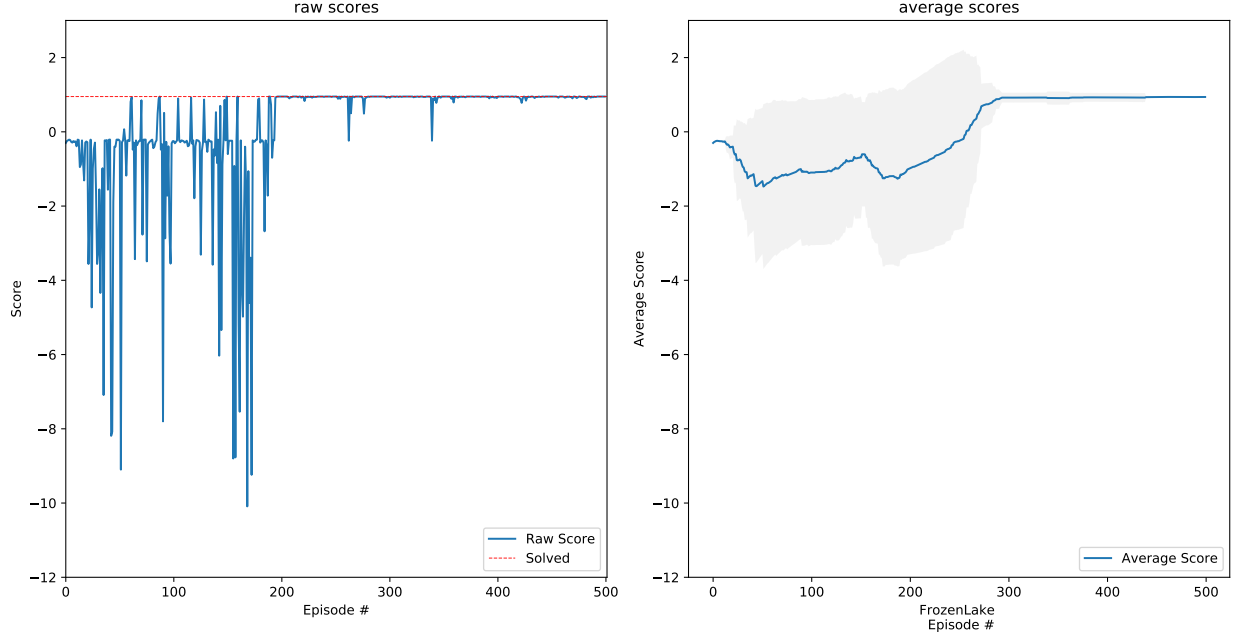


Figure 3: **Variational quantum circuit for Deep Q Learning** The figure shows our proposed DQL-agent reach the optimal policy with a total reward of 0.9 at the 198th iteration. The gray area in the figure represents the standard deviation of reward in each iteration during exploration with the standard reinforcement learning reproducible setting [34] for stability. The policy learned via Quantum Circuit becomes more stable after the 301st iteration.

Table 2: Comparison of Classical Reinforcement Learning Algorithms with Discrete Action Space

Algorithm	Policy	Action Space	State Space	Operator	Complexity of Parameters
Monte Carlo	Off-policy	Discrete	Discrete	Sample-means	$\mathcal{O}(n^3)$
Q-Learning	Off-policy	Discrete	Discrete	Q-value	$\mathcal{O}(n^3)$
SARSA	On-policy	Discrete	Discrete	Q-value	$\mathcal{O}(n^3)$
DQN	Off-policy	Discrete	Continuous	Q-value	$\mathcal{O}(n^2)$
VQ-DQN <sup>2</sup>	Off-policy	Quantum	Quantum	Q-value	$\mathcal{O}(n)$
VQ-DQN <sup>1</sup>	Off-policy	Quantum	Quantum	Q-value	$\mathcal{O}(\log n)$

### 3.5 Quantum Advantage on Memory Consumption

In our proposed method, the quantum advantage refers to the memory consumption, which means there are much less parameters in the quantum circuits. The quantum advantage in terms of the parameters of the quantum circuit relies on the data encoding schemes. For example, as to an amplitude coding, the number of parameters is  $\text{poly}(\log N)$  in contrast to  $\text{poly}(N)$  in a standard neural network<sup>1</sup>. However, computational basis encoding involves  $N$  parameters in our proposed quantum RL,  $N^2$  parameters in neural network based RL, and  $N^3$  in tabular  $Q$ -learning, where  $N$  is the dimension of input vectors<sup>2</sup>. In the Frozen-Lake environment, the number of parameters in our proposed variational quantum circuit based RL is 28, while in tabular  $Q$ -Learning, the table needs to store all the state-action information is of the size  $16 \times 4 = 64$ , which reduces the parameters as a rate of  $(64 - 28)/64 = 56.25\%$ . In the Cognitive-Radio environment with  $N$  possible channels, the parameter numbers are separately  $N \times (3 \times 2 + 1)$  in our quantum circuit based RL,  $2 \times N^2 + 2 \times N$  in neural network based RL, and  $N^3$  in tabular  $Q$ -learning method. By comparison, the parameters of our proposed method grows linearly with the dimension of the input vector, which is shown in Figure6.

<sup>1</sup>VQ-DQN with amplitude encoding can harvest full logarithmic less parameters compared with classical models.

<sup>2</sup>The number of parameters in VQ-DQN with computational basis encoding grows only linearly with the dimension of the input vector  $n$ .

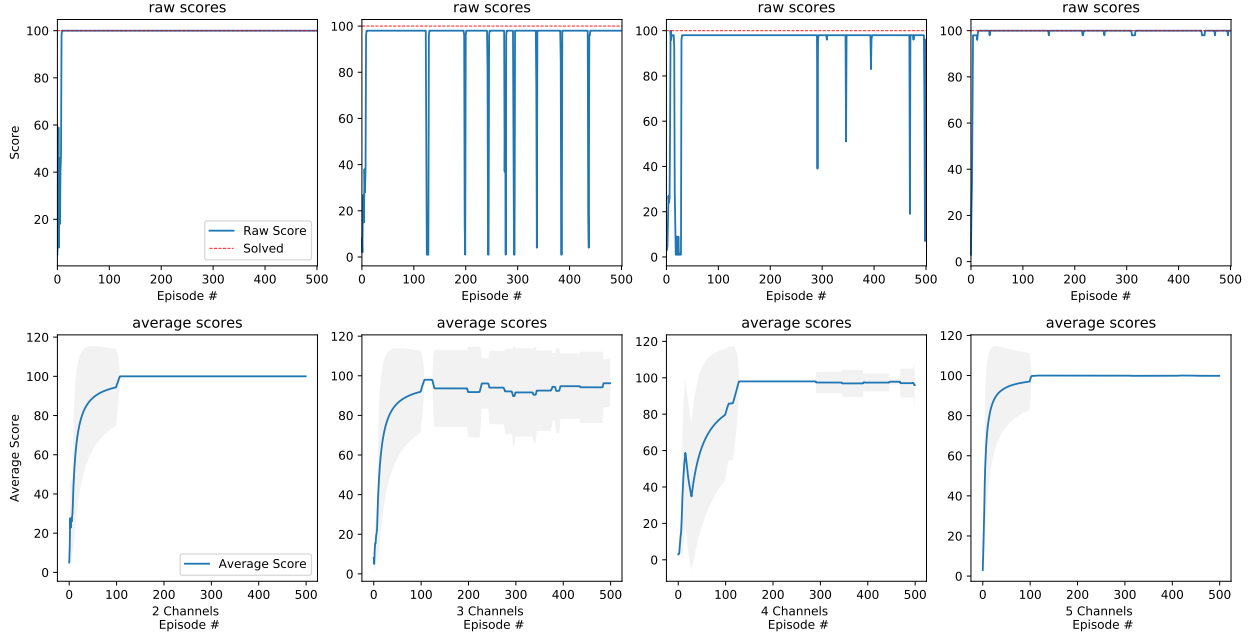


Figure 4: **Variational quantum circuit for Deep Q Learning on Cognitive-Radio** In the Cognitive-Radio experiments, we limit the maximum steps an agent can run to 100, and the reward scheme is that for each correct choice of the channel, the agent will get a +1 reward and -1 for incorrect selection. The maximum reward an agent can achieve under this setting is 100. The figure shows our proposed DQL-agent reach the optimal policy with a total reward of 100 in the 2-Channel and 5-Channel case at only several iterations. For the case of 3-Channel and 4-Channel, the agent also reach near-optimal policy at only several iterations. The gray area in the figure represents the standard deviation of reward in each iteration during exploration with the standard reinforcement learning reproducible setting [34] for stability. The policy learned via Variational Quantum Circuits becomes more stable after around 100 iterations for all four cases.

Table 3: Comparison of Number of Parameters in Classical Q-Learning and Quantum Deep Reinforcement Learning

Env.	2-Channels	3-Channels	4-Channels	5-Channels	Frozen-Lake
Q-Learning	$2 \times 2 \times 2$	$3 \times 3 \times 3$	$4 \times 4 \times 4$	$5 \times 5 \times 5$	$4 \times 4 \times 4$
VQ-DQN	$2 \times (3 \times 2 + 1)$	$3 \times (3 \times 2 + 1)$	$4 \times (3 \times 2 + 1)$	$5 \times (3 \times 2 + 1)$	$4 \times (3 \times 2 + 1)$

## 4 Discussions

### 4.1 Overview of Quantum Machine Learning

A general review of the field *quantum machine learning* can refer to [35] and [36]. As for *quantum reinforcement learning*, [37, 38] have proposed a framework called *projective simulation*. The key concept in this setting is that the *agent* keeps a *memory* of the transition history. Before executing each action, the agent will *simulate* several possible outcomes according to historical data stored in the memory. It is conceptually related to the well-known Monte-Carlo Tree Search [7, 39] and it is interesting to investigate the quantum counterparts and possible quantum advantages.

### 4.2 Empirical Applications on a Multi-channel Radio Network

We further extend our VQ-DQN on a classical spectrum control problem in cognitive radio, with the ns3-gym [30] environment. We consider the problem of radio channel selection in a wireless multi-channel environment, e.g. 802.11 networks with external interference. We first create a scalable reinforcement learning environment sim-radio-spectrum (SRS) with a customized state and an action echo in a real multi-channel spectrum scenario. The objective of the agent selects a channel free of interference of the next time slot. We consider a simple illustrative example where the external interference follows a periodic pattern, i.e. sweeping over all channels one to four in the same order as shown in the



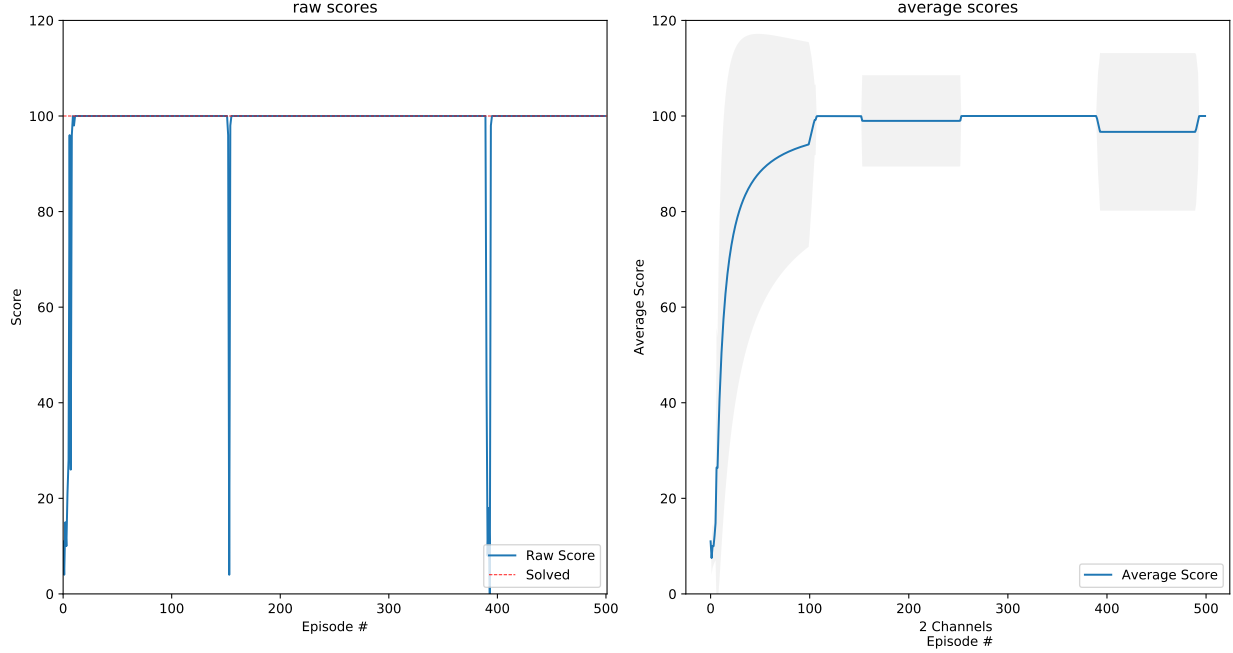


Figure 5: **Variational quantum circuit for Deep Q Learning on Cognitive-Radio with IBM Qiskit Aer Quantum Simulator and noise from the real Quantum machine** In this experiment, we investigated the robustness of the VQ-DQN against the noise in quantum machines. The device noise is downloaded from remote real quantum machines and then incorporated with the simulator software qiskit-aer provided by IBM. This noisy backend then replaced the noiseless backend in previous experiments. The experiment shows that our proposed variational quantum circuit based DQN is robust against noise in current quantum machines.

Figure 3. This extra environment offer a feasible test-bed for quantum RL with desirable self-defined environment with a lower action and space complexity working in the NISQ.

Our proposed quantum reinforcement learning environment on radio-channel-access network included:

- *State* –  $ns3$  statistics with the radio channels capacity, with a customized channel number =  $N$ . (e.g., a state of  $[1\ 0\ 0\ 0]$  represents for  $N = 4$  channel and a primary user on the 1st channel.)
- *Action* – selecting one channel for the secondary accessing a radio channel out of  $N$  channels.
- *Reward* –  $-1$  for a collision with the primary user;  $+1$  for no collision.
- *Info* – Boolean format of terminal when radio learning agent(s) faces to collision more than three times.

Different with the benchmark environments of complex reinforcement learning like Atari games. Our environments require much more qubits for conducting simulations. Although it can be encoded with computational basis encoding or amplitude encoding, the number of qubits needed is intractable for numerical simulations on classical computers and also exceed commercially available quantum devices. We could further investigate these complex RL environments with the same setting proposed in this work when large quantum machines are released.

### 4.3 Future Work: Amplitude Encoding Scheme

Unlike an amplitude encoding, the computational basis encoding has not fully employed the quantum advantages. Although in a constraint condition of quantum simulators, we can verify the feasibility of applying quantum circuits for resolving deep reinforcement learning problems. The related empirical results suggest that the quantum advantages outperform both tabular  $Q$ -learning and neural network based RL. To obtain the ideal quantum circuits with significantly less parameters, we apply *amplitude encoding* to reduce the complexity of parameters as small as  $\text{poly}(\log N)$  in contrast to a standard neural network with  $\text{poly}(N)$  parameters. Future work includes an investigation of applying variational quantum circuits to represent the high-dimensional data under complicated environment.

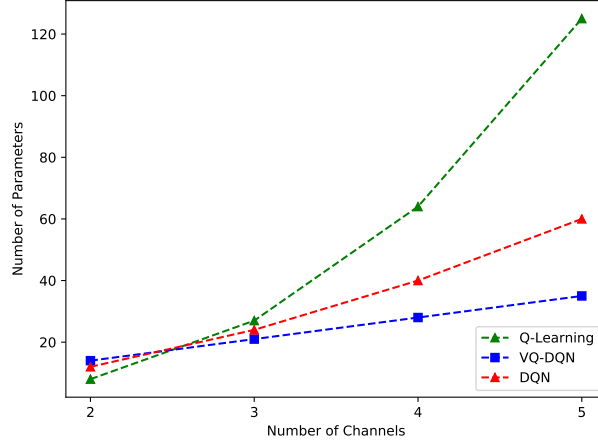


Figure 6: **Comparison of Memory Consumption in different learning scheme** The figure shows our proposed DQL-agent has the quantum advantage in memory consumption compared to classical  $Q$ -learning and Deep  $Q$ -learning. Specifically, in our cognitive radio channel selection experiment, we set up four different testing environment, with 2,3,4,5 possible channels respectively. With the classical  $Q$ -learning, the number of parameters grow with  $n^3$  and in Deep  $Q$ -learning the number of parameters grow with  $n^2$ , however, with our proposed variational quantum circuit based RL, the number of parameter grows as  $n \times (3 \times 2 + 1)$  only.

## 5 Conclusions

This is the first demonstration of variational quantum circuits to approximate the deep  $Q$ -value function with experience replay and target network. Our proposed framework shows that the quantum advantage in terms of less memory consumption and the reduction of model parameters. Specifically, the variational quantum deep  $Q$ -learning involves parameters as small as  $\mathcal{O}(n)$ , but the tabular  $Q$ -learning and neural network based deep  $Q$ -learning have  $\mathcal{O}(n^3)$  and  $\mathcal{O}(n^2)$  parameters, respectively.

## 6 Acknowledgements

Thanks to Prof. Yun-Cheng Tsai for constructive discussion and great support. Thanks to Cheng-Lin Hong for helping on setting computational clusters.

## References

- [1] Yann LeCun, Yoshua Bengio, and Geoffrey Hinton. Deep learning. *nature*, 521(7553):436, 2015.
- [2] Karen Simonyan and Andrew Zisserman. Very deep convolutional networks for large-scale image recognition. *arXiv preprint arXiv:1409.1556*, 2014.
- [3] Christian Szegedy, Wei Liu, Yangqing Jia, Pierre Sermanet, Scott Reed, Dragomir Anguelov, Dumitru Erhan, Vincent Vanhoucke, and Andrew Rabinovich. Going deeper with convolutions. In *Proceedings of the IEEE conference on computer vision and pattern recognition*, pages 1–9, 2015.
- [4] Athanasios Voulodimos, Nikolaos Doulamis, Anastasios Doulamis, and Eftychios Protopapadakis. Deep Learning for Computer Vision: A Brief Review. *Computational Intelligence and Neuroscience*, 2018:1–13, 2018.
- [5] Ilya Sutskever, Oriol Vinyals, and Quoc V Le. Sequence to sequence learning with neural networks. In *Advances in neural information processing systems*, pages 3104–3112, 2014.
- [6] Yiming Kong, Hui Zang, and Xiaoli Ma. Improving tcp congestion control with machine intelligence. In *Proceedings of the 2018 Workshop on Network Meets AI & ML*, pages 60–66. ACM, 2018.
- [7] David Silver, Aja Huang, Chris J. Maddison, Arthur Guez, Laurent Sifre, George van den Driessche, Julian Schrittwieser, Ioannis Antonoglou, Veda Panneershelvam, Marc Lanctot, Sander Dieleman, Dominik Grewe, John Nham, Nal Kalchbrenner, Ilya Sutskever, Timothy Lillicrap, Madeleine Leach, Koray Kavukcuoglu, Thore Graepel, and Demis Hassabis. Mastering the game of Go with deep neural networks and tree search. *Nature*, 529(7587):484–489, 1 2016.

- [8] Artem Borin and Dmitry A Abanin. Approximating power of machine-learning ansatz for quantum many-body states. *arXiv preprint arXiv:1901.08615*, 2019.
- [9] Giuseppe Carleo, Kenny Choo, Damian Hofmann, James ET Smith, Tom Westerhout, Fabien Alet, Emily J Davis, Stavros Efthymiou, Ivan Glasser, Sheng-Hsuan Lin, et al. Netket: A machine learning toolkit for many-body quantum systems. *arXiv preprint arXiv:1904.00031*, 2019.
- [10] Giuseppe Carleo, Ignacio Cirac, Kyle Cranmer, Laurent Daudet, Maria Schuld, Naftali Tishby, Leslie Vogt-Maranto, and Lenka Zdeborová. Machine learning and the physical sciences. *arXiv preprint arXiv:1903.10563*, 2019.
- [11] Askery Canabarro, Felipe Fernandes Fanchini, André Luiz Malvezzi, Rodrigo Pereira, and Rafael Chaves. Unveiling phase transitions with machine learning. *arXiv preprint arXiv:1904.01486*, 2019.
- [12] Zheng An and DL Zhou. Deep reinforcement learning for quantum gate control. *arXiv preprint arXiv:1902.08418*, 2019.
- [13] Emmanuel Flurin, Leigh S Martin, Shay Hacohen-Gourgy, and Irfan Siddiqi. Using a recurrent neural network to reconstruct quantum dynamics of a superconducting qubit from physical observations. *arXiv preprint arXiv:1811.12420*, 2018.
- [14] Philip Andreasson, Joel Johansson, Simon Liljestrand, and Mats Granath. Quantum error correction for the toric code using deep reinforcement learning. *arXiv preprint arXiv:1811.12338*, 2018.
- [15] Hendrik Poulsen Nautrup, Nicolas Delfosse, Vedran Dunjko, Hans J Briegel, and Nicolai Friis. Optimizing quantum error correction codes with reinforcement learning. *arXiv preprint arXiv:1812.08451*, 2018.
- [16] Andrew Cross. The ibm q experience and qiskit open-source quantum computing software. In *APS Meeting Abstracts*, 2018.
- [17] Trevor Lanting, Anthony J Przybysz, A Yu Smirnov, Federico M Spedalieri, Mohammad H Amin, Andrew J Berkley, Richard Harris, Fabio Altomare, Sergio Boixo, Paul Bunyk, et al. Entanglement in a quantum annealing processor. *Physical Review X*, 4(2):021041, 2014.
- [18] Daniel Gottesman. Stabilizer codes and quantum error correction. *arXiv preprint quant-ph/9705052*, 1997.
- [19] Daniel Gottesman. Theory of fault-tolerant quantum computation. *Physical Review A*, 57(1):127, 1998.
- [20] Kosuke Mitarai, Makoto Negoro, Masahiro Kitagawa, and Keisuke Fujii. Quantum circuit learning. *Physical Review A*, 98(3):032309, 2018.
- [21] Yuxuan Du, Min-Hsiu Hsieh, Tongliang Liu, and Dacheng Tao. The expressive power of parameterized quantum circuits. *arXiv preprint arXiv:1810.11922*, 2018.
- [22] Ian Goodfellow, Jean Pouget-Abadie, Mehdi Mirza, Bing Xu, David Warde-Farley, Sherjil Ozair, Aaron Courville, and Yoshua Bengio. Generative adversarial nets. In *Advances in neural information processing systems*, pages 2672–2680, 2014.
- [23] Richard S. Sutton and Andrew G. Barto. *Reinforcement learning : an introduction*.
- [24] Volodymyr Mnih, Adrià Puigdomènech Badia, Mehdi Mirza, Alex Graves, Timothy P. Lillicrap, Tim Harley, David Silver, and Koray Kavukcuoglu. Asynchronous Methods for Deep Reinforcement Learning. 2 2016.
- [25] Volodymyr Mnih, Koray Kavukcuoglu, David Silver, Andrei A. Rusu, Joel Veness, Marc G. Bellemare, Alex Graves, Martin Riedmiller, Andreas K. Fidjeland, Georg Ostrovski, Stig Petersen, Charles Beattie, Amir Sadik, Ioannis Antonoglou, Helen King, Dharshan Kumaran, Daan Wierstra, Shane Legg, and Demis Hassabis. Human-level control through deep reinforcement learning. *Nature*, 518(7540):529–533, 2 2015.
- [26] Edward Farhi and Hartmut Neven. Classification with quantum neural networks on near term processors. *arXiv preprint arXiv:1802.06002*, 2018.
- [27] Maria Schuld, Alex Bocharov, Krysta Svore, and Nathan Wiebe. Circuit-centric quantum classifiers. *arXiv preprint arXiv:1804.00633*, 2018.
- [28] Maria Schuld, Ville Bergholm, Christian Gogolin, Josh Izaac, and Nathan Killoran. Evaluating analytic gradients on quantum hardware. *Physical Review A*, 99(3):032331, 3 2019.
- [29] Maria Schuld and Francesco Petruccione. Information encoding. In *Supervised Learning with Quantum Computers*, pages 139–171. Springer International Publishing, Cham, 2018.
- [30] Piotr Gawłowicz and Anatolij Zubow. ns3-gym: Extending openai gym for networking research. *arXiv preprint arXiv:1810.03943*, 2018.

- [31] Ville Bergholm, Josh Izaac, Maria Schuld, Christian Gogolin, and Nathan Killoran. PennyLane: Automatic differentiation of hybrid quantum-classical computations. *arXiv preprint arXiv:1811.04968*, 2018.
- [32] Adam Paszke, Sam Gross, Soumith Chintala, Gregory Chanan, Edward Yang, Zachary DeVito, Zeming Lin, Alban Desmaison, Luca Antiga, and Adam Lerer. Automatic differentiation in pytorch. 2017.
- [33] Greg Brockman, Vicki Cheung, Ludwig Pettersson, Jonas Schneider, John Schulman, Jie Tang, and Wojciech Zaremba. Openai gym. *arXiv preprint arXiv:1606.01540*, 2016.
- [34] Joelle Pineau, G Fried, RN Ke, and H Larochelle. Iclr 2018 reproducibility challenge. In *ICML workshop on Reproducibility in Machine Learning*, 2018.
- [35] Vedran Dunjko and Hans J Briegel. Machine learning & artificial intelligence in the quantum domain: a review of recent progress. *Reports on Progress in Physics*, 81(7):074001, 7 2018.
- [36] Vedran Dunjko, Jacob M. Taylor, and Hans J. Briegel. Advances in quantum reinforcement learning. In *2017 IEEE International Conference on Systems, Man, and Cybernetics (SMC)*, pages 282–287. IEEE, 10 2017.
- [37] Hans J. Briegel and Gemma De las Cuevas. Projective simulation for artificial intelligence. *Scientific Reports*, 2(1):400, 12 2012.
- [38] Julian Mautner, Adi Makmal, Daniel Manzano, Markus Tiersch, and Hans J. Briegel. Projective Simulation for Classical Learning Agents: A Comprehensive Investigation. *New Generation Computing*, 33(1):69–114, 1 2015.
- [39] David Silver, Julian Schrittwieser, Karen Simonyan, Ioannis Antonoglou, Aja Huang, Arthur Guez, Thomas Hubert, Lucas Baker, Matthew Lai, Adrian Bolton, Yutian Chen, Timothy Lillicrap, Fan Hui, Laurent Sifre, George van den Driessche, Thore Graepel, and Demis Hassabis. Mastering the game of Go without human knowledge. *Nature*, 550(7676):354–359, 10 2017.